



The emerging contaminant 3,3'-dichlorobiphenyl (PCB-11) impedes Ahr activation and Cyp1a activity to modify embryotoxicity of Ahr ligands in the zebrafish embryo model (*Danio rerio*)[☆]

Monika A. Roy^{a, b}, Karilyn E. Sant^{a, 1}, Olivia L. Venezia^a, Alix B. Shipman^a,
Stephen D. McCormick^c, Panithi Saktrakulkla^d, Keri C. Hornbuckle^e,
Alicia R. Timme-Laragy^{a, *}

^a Department of Environmental Health Sciences, University of Massachusetts Amherst, Amherst, MA 01003, USA

^b Biotechnology Training Program, University of Massachusetts Amherst, Amherst, MA 01003, USA

^c US Geological Survey, Leetown Science Center, S.O. Conte Anadromous Fish Research Laboratory, Turners Falls, MA 01376, USA

^d Interdisciplinary Graduate Program in Human Toxicology, University of Iowa, Iowa City, IA 52242, USA

^e Department of Civil and Environmental Engineering and IIHR-Hydroscience and Engineering, University of Iowa, Iowa City, IA 52242, USA

ARTICLE INFO

Article history:

Received 24 April 2019

Received in revised form

29 July 2019

Accepted 4 August 2019

Available online 6 August 2019

Keywords:

PCB-11

3,3'-dichlorobiphenyl

Aryl hydrocarbon receptor (Ahr) pathway

Developmental toxicity

Mixtures

Danio rerio

ABSTRACT

3,3'-dichlorobiphenyl (PCB-11) is an emerging PCB congener widely detected in environmental samples and human serum, but its toxicity potential is poorly understood. We assessed the effects of three concentrations of PCB-11 on embryotoxicity and Aryl hydrocarbon receptor (Ahr) pathway interactions in zebrafish embryos (*Danio rerio*). Wildtype AB or transgenic *Tg(gut:GFP)* strain zebrafish embryos were exposed to static concentrations of PCB-11 (0, 0.2, 2, or 20 μ M) from 24 to 96 h post fertilization (hpf), and gross morphology, Cytochrome P4501a (Cyp1a) activity, and liver development were assessed via microscopy. Ahr interactions were probed via co-exposures with PCB-126 or beta-naphthoflavone (BNF). Embryos exposed to 20 μ M PCB-11 were also collected for PCB-11 body burden, qRT-PCR, RNAseq, and histology. Zebrafish exposed to 20 μ M PCB-11 absorbed 0.18% PCB-11 per embryo at 28 hpf and 0.61% by 96 hpf, and their media retained 1.36% PCB-11 at 28 hpf and 0.84% at 96 hpf. This concentration did not affect gross morphology, but altered the transcription of xenobiotic metabolism and liver development genes, impeded liver development, and increased hepatocyte vacuole formation. In co-exposures, 20 μ M PCB-11 prevented deformities caused by PCB-126 but exacerbated deformities in co-exposures with BNF. This study suggests that PCB-11 can affect liver development, act as a partial agonist/antagonist of the Ahr pathway, and act as an antagonist of Cyp1a activity to modify the toxicity of compounds that interact with the Ahr pathway.

© 2019 Elsevier Ltd. All rights reserved.

1. Introduction

The emerging polychlorinated biphenyl (PCB) congener 3,3'-dichlorobiphenyl (PCB-11) has been identified as a non-legacy, non-Aroclor PCB inadvertently generated during the commercial

production of diarylide azo-type pigments used in consumer goods such as paper and plastic products (Rodenburg et al., 2010; Shang et al., 2014). It is thought that PCB-11 is mobilized into water sources via wastewater discharge during pigment manufacturing, and when consumer goods containing these pigments are discarded or recycled (Du et al., 2008; Rodenburg et al., 2011; Rodenburg et al., 2015). PCB-11 also volatilizes from paints and resins and can enter the body through inhalation exposures (Herkert et al., 2018; Shanahan et al., 2015). Additionally, PCB-11 has been detected in food sources such as commercial cow's milk (Chen et al., 2017), and both PCB-11 and its sulfate metabolite have been detected in human serum (Grimm et al., 2017; Koh et al., 2015), including in pregnant women (0.005–1.717 μ g/L) (Sethi et al.,

[☆] This paper has been recommended for acceptance by Charles Wong.

* Corresponding author. Department of Environmental Health Sciences, University of Massachusetts Amherst, 686 N. Pleasant St. Goessmann 171, Amherst, MA 01003, USA.

E-mail address: aliciat@umass.edu (A.R. Timme-Laragy).

¹ Division of Environmental Health, San Diego State University, 5500 Campanile Dr., San Diego, CA 92182, USA.

2017), demonstrating an exposure risk in the fetal environment. Despite growing evidence of human exposures, little is known about PCB-11 toxicity, particularly for the highly-sensitive period of embryonic development. To investigate this knowledge gap, we used the zebrafish embryo model to assess developmental toxicity, with a focus on potential interactions with the Aryl hydrocarbon receptor (Ahr) pathway.

The Ahr is a basic-helix-loop-helix/per-Arnt-Sim (bHLH/PAS) transcription factor family member that is activated by both naturally occurring and synthetic ligands like polycyclic aromatic hydrocarbons (PAHs) and dioxin-like PCBs (Huang et al., 1993). The Ahr is constitutively expressed, but upon ligand binding, translocates from the cytosol to the nucleus where it forms a heterodimer with the Aryl hydrocarbon receptor nuclear translocator (Arnt) (Reisz-Porszasz et al., 1994). The Ahr/Arnt heterodimer then binds to Xenobiotic Response Elements (XREs) in promoter regions of Ahr-responsive genes (Coumailleau et al., 1995; Sojka et al., 2000), increasing production of enzymes that can biotransform the Ahr ligands in Phase I and Phase II metabolism (Kuhnert et al., 2017; Nakayama et al., 2008). Zebrafish and human Ahr pathway activation is similar, but it is important to note that while zebrafish have three Ahr gene isoforms (*ahr1a*, *ahr1b*, and *ahr2*) (Karchner et al., 2005), toxicity effects have been shown to be primarily mediated by *ahr2* (Billiard et al., 2006; Carney et al., 2006; Jonsson et al., 2007a).

Upon Ahr pathway activation, many ligands are substrates for biotransformation by the Cyp1a enzyme, and are most often converted to more hydrophilic metabolites for excretion (Nebert et al., 2004). However, not all Ahr ligands are good substrates for Cyp1a biotransformation. For instance, the dioxin-like PCB-126 activates the Ahr pathway and upregulates Cyp1a activity, but exerts toxicity independent of Cyp1a (Billiard et al., 2006; Jonsson et al., 2012; Timme-Laragy et al., 2007); in zebrafish embryos PCB-126 exposure results in a suite of deformities including pericardial edema, craniofacial malformations, and impaired yolk sac utilization. This toxicity is rescued only when *ahr2* activation is blocked by either antagonizing the receptor or by genetic means to either knock-out or knock-down the receptor (Billiard et al., 2006). For ligands that are good substrates for Cyp1a metabolism, another route to toxicity involves blocked Cyp1a biotransformation processes, where unmetabolized ligands can continue to activate the Ahr, resulting in enhanced toxicity (Billiard et al., 2006; Timme-Laragy et al., 2007; Wincent et al., 2016; Zhao et al., 2013). Cyp1a induction in zebrafish is similar as in humans (Goldstone et al., 2007; Jonsson et al., 2007b; Nebert et al., 2004; Scornaienchi et al., 2010), and this enzymatic activity can be measured using the well-established *in vivo* ethoxyresorufin-O-deethylase (EROD) bioassay (Billiard et al., 2006; Nacci et al., 2005) as a useful tool to investigate the potential toxicity of emerging contaminants that might act through the Ahr (Boehler et al., 2018; Kais et al., 2018).

The environmental presence of PCB-11 is likely to continue, and increase, through the production of diarylide pigments and the recycling of consumer products, but little research has been conducted to understand the molecular interactions and health implications for any quantity of PCB-11. Our objectives for this study were to use the zebrafish model to test a range of concentrations to understand the molecular actions of PCB-11, and how it influences morphological development and xenobiotic metabolism. In addition to examining the effects of single exposures of PCB-11, we took a mixture approach to understand whether PCB-11 can influence the effects of well-established Ahr activators, such as PAHs, that are likely to exist in urban locations where PCB-11 has been detected in air and water samples (Hu et al., 2008; Rodenburg et al., 2011; Shanahan et al., 2015). We used the EROD bioassay to monitor Cyp1a enzyme activity, fluorescence imaging techniques to look at

liver development, and paired this with Ahr-related gene transcription levels, RNAseq, and histology as tools to explore whether this emerging contaminant is a public health concern. Our findings indicate that PCB-11 interacts with the Ahr pathway, impedes liver development, and perturbs pathways related to lipid metabolism, but in co-exposures with other Ahr agonists can more significantly either suppress or exacerbate toxicological outcomes, depending on the co-exposure.

2. Materials and methods

2.1. Animal care

Adult wildtype AB and transgenic *Tg(gut:GFP)* zebrafish (*Danio rerio*) were housed on a 14 h light:10 h dark cycle in a recirculating Aquaneering system (San Diego, CA) maintained at 28.5 °C. Embryos were obtained from breeding groups of 40 fish with a 2:1 female:male ratio. Embryos were collected at 1 h post fertilization (hpf), washed, and stored at low density in 0.3x Danieau's media [17 mM NaCl, 2 mM KCl, 0.12 mM MgSO₄, 1.8 mM Ca(NO₃)₂, 1.5 mM HEPES, pH 7.6] in an incubator with the same temperature and light conditions as the adult fish. At 24 hpf, embryos were staged and screened for normal development before use in experiments. All animal care and experiments were conducted in accordance with protocols approved by the University of Massachusetts Amherst Institutional Animal Care and Use Committee (IACUC; Animal Welfare Assurance Number A3551-01). Animals were treated humanely with due consideration to the alleviation of stress and discomfort.

2.2. Chemicals

PCB-126 and PCB-11 were from Ultra Scientific (North Kingstown, RI), beta-naphthoflavone (BNF) from Fisher Scientific (Pittsburg, PA), and 7-ethoxyresorufin-O-deethylase (7-ER) from MP Biomedicals (Solon, OH). All chemicals were dissolved in 100% dimethyl sulfoxide (DMSO) from Fisher Scientific (Fair Lawn, NJ). Stock solutions were stored at -20 °C in glass amber vials, and were fully thawed and vortexed before use. For zebrafish concentration analyses, PCB-13 was used as a surrogate standard (SS) from AccuStandard (New Haven, CT), d5-PCB-30 was used as an internal standard (IS) from Cambridge Isotope Laboratories (Andover, MA), and pesticide-grade hexane was used from Fisher Chemical (Beersse, Belgium).

2.3. PCB-11 concentration analysis

The lowest PCB-11 concentration of 0.2 μM used in this study was selected based on previous studies that measured aqueous "whole water" (dissolved and particle phase) concentrations of PCB-11 near industrial effluents (Litten et al., 2002; Rodenburg et al., 2010; Rodenburg et al., 2015) and in marine species (Addison et al., 1999; Pizzini et al., 2017; Zhu et al., 2015). We included concentrations one and two orders of magnitude higher in our experiments based on concentrations of PCB-11 used in previously in a rodent model (Sethi et al., 2017). PCB-11 adheres to surfaces and particles, but as a lower-chlorinated congener, readily volatilizes (Agency for Toxic Substances and Disease Registry, 2000). The solubility of PCB-11 in water is 354 μg/L (Dunnivant et al., 1988) and its octanol-water partition coefficient is log 5.28 (International Agency for Research on Cancer, 2016). The concentrations of PCB-11 used in this study are of the dissolved phase only of PCB-11 in water. In order to dissolve the middle and highest concentrations of PCB-11 used in this study (2 μM and 20 μM) into an aqueous medium, DMSO was used. In order to understand the

amount of PCB-11 that was taken up into the zebrafish larval tissue, embryos were analyzed at 28 hpf (4 h after the exposure began) and at 96 hpf (end of exposure period) at the University of Iowa for whole organism tissue and media analysis of the highest concentration of PCB-11 (20 μ M), described in Supplemental Method 1. The PCB-11 concentration analysis temperature programs and ion transitions for this analysis can be found in [Supplemental Table 1](#).

2.4. Chemical exposures

At 24 hpf, zebrafish embryos were manually dechorionated using Watchmakers forceps. For all experiments, five embryos were exposed in 5 mL of 0.3x Danieau's water in 20 mL glass scintillation vials, with at least 2 technical replicates per exposure group per experiment. Zebrafish were statically exposed from 24 to 96 hpf to three PCB-11 concentrations (0.2, 2, or 20 μ M) or DMSO, either alone for single exposure experiments or in combination with either PCB-126 or BNF for co-exposure experiments. This time frame was chosen since *ahr2* expression in zebrafish does not become constant until 24 hpf, a time point when *cyp1a* also starts to express ([Andreasen et al., 2002](#)). Previous developmental toxicity experiments with exposures starting at 24 hpf have also shown that both PCB-126 and BNF activate the Ahr pathway and cause deviations in morphological development, either alone or in co-exposures ([Garner et al., 2013](#); [Timme-Laragy et al., 2007](#)). For experiments with PCB-126, a final concentration of 5 nM was used, shown previously to cause malformations in zebrafish ([Rousseau et al., 2015](#)). For experiments with BNF, concentrations of either 184 nM (50 μ g/L) or 367 nM (100 μ g/L) were used, shown previously to induce Ahr-related gene activity in zebrafish ([Timme-Laragy et al., 2007](#)). For EROD experiments, each vial contained 0.5 μ g/L of 7-ER, which was added at 24 hpf when dosing occurred. All vials contained a total DMSO concentration of 0.05% v/v, and all exposures were static between 24 and 96 hpf. Liver development experiments used *Tg(gut:GFP)* embryos, which express GFP in liver tissue starting at about 22 hpf and is regulated through *ef1a* ([Field et al., 2003](#)), in place of AB embryos. EROD, liver development, qRT-PCR, and RNAseq experiments were repeated at least 3 times, and experiments for histology endpoints were repeated twice.

2.5. Microscopy and image analysis

At 96 hpf, live larvae were sedated by a 10 s exposure to 2% v/v MS-222 solution (prepared as 4 mg/mL tricaine powder in water, pH buffered, and stored at -20° C until thawed for use) before being mounted on individual 3% methylcellulose drops in a left-lateral orientation. For EROD imaging experiments, AB larvae were imaged on an upright Olympus compound fluorescence microscope custom modified by Kramer Scientific (Amesbury, MA) and equipped with an Axiocam 503 camera (Carl Zeiss Inc., Thornwood, NY) and an 89 North® PhotoFluor® II light source (89 North®, Burlington, VT). For liver development experiments, *Tg(gut:GFP)* larvae were imaged *in vivo* on a Zeiss Stereo Axio Zoom.V16 (Carl Zeiss Inc.). All measurements for zebrafish length, EROD light intensity, and liver area were measured with the Zen Lite program (Carl Zeiss Inc.). Since pericardial edema is a characteristic outcome of fish embryos exposed to halogenated aromatic compounds ([King-Heiden et al., 2012](#)) like PCB-126, pericardial area was measured on all fish as a quantitative measurement to represent overall deformities. For all experiments, transmitted bright-field microscopy images of the whole fish and gut region were taken with 2x and 10x objectives, and liver/gut area was captured with a 10x objective on either an RFP filter for EROD experiments or GFP filter for liver development experiments.

2.6. qRT-PCR

For all qRT-PCR experiments, at 96 hpf zebrafish larvae were collected and pooled in groups of 10–15 larvae after exposure, and preserved in RNAlater (Thermo Fisher Scientific, Waltham, MA) at -80° C. Zebrafish larvae were thawed, transferred to lysis buffer, and sonicated by pulsing 3 times with an Emerson Industrial Branson Sonifier® (Danbury, CT). RNA isolation was performed using 2-Mercaptoethanol (MP Biomedicals) and a GeneJET RNA Purification Kit (Thermo Fisher Scientific) following manufacturer instructions. RNA quantity and quality was assessed using a Bio-Drop μ LITE spectrophotometer (Cambridge, United Kingdom). Sample cDNA was prepared using an iScript reaction mix kit (Bio-Rad, Hercules, CA), diluted 1:9 with nuclease-free water, and stored at -80° C until processing. Each qRT-PCR sample was prepared using 10 μ L of 2X iQ SYBR® Green Supermix (Bio-Rad), 5 pM each of forward and reverse primers (1 μ L total), 5 μ L of nuclease-free water, and 4 μ L (1 ng) of cDNA. Samples were run on 96-well plates in a CFX Connect Real-Time PCR Detection System (Bio-Rad), and samples were analyzed using the CFX Manager software (Bio-Rad). qRT-PCR was carried out in duplicate for the aryl hydrocarbon receptor 2 (*ahr2*) and cytochrome p4501A1 (*cyp1a*) genes. The β -actin (*actb*) gene was used as a housekeeping gene, and its transcription did not change significantly across exposure groups. The β 2-Microglobulin (*b2m*) gene was used to verify gene transcription levels (data not shown). All gene primer sequences can be found in [Supplemental Table 2](#).

2.7. RNAseq and analysis

At 96 hpf, triplicate pools of 18–20 zebrafish larvae exposed to either DMSO or 20 μ M PCB-11 were collected for RNAseq and transferred to the UMass Amherst Genomics Resource Laboratory. Details on RNAseq library preparation and next-generation sequencing are in Supplemental Method 2. RNAseq data has been deposited into the NCBI Gene Expression Omnibus (GEO) database with the accession number GSE118955. Gene ontology and pathway analysis was performed on the Gene Set Enrichment Analysis (GSEA) platform (Broad Institute, Massachusetts Institute of Technology, and Regents of the University of California) using the Kyoto Encyclopedia of Genes and Genomes (KEGG) gene sets database. Gene ontology and pathway analysis was also performed using LPath (<http://lpath.ncibi.org/>), which used logistic regression to calculate KEGG pathways significantly up or down-regulated by PCB-11 exposure ([Kim et al., 2012](#)).

2.8. Histology

At 96 hpf, zebrafish exposed to either DMSO or 20 μ M PCB-11 ($n=4$ fish for both groups), were fixed in 4% v/v paraformaldehyde (Alfa Aesar, Tewksbury, MA) and preserved in 70% ethanol at 4° C until processing. Fixed samples were sent to the UMass Medical School Morphology Core (Worcester, MA), where they underwent tissue processing on a Shandon Citadel 2000 (Thermo Fisher) and then were paraffin embedded 3–4 per cassette using a Sakura Tissue-Tek (Torrance, CA). The paraffin blocks were sectioned along the midlines of the zebrafish in a sagittal orientation to facilitate liver examination, and ten sections were mounted and stained with hematoxylin and eosin (H&E) according to standard protocols. At UMass Amherst, all sections were imaged at 40x magnification on an EVOS FL Auto Microscope (Thermo Fisher Scientific) and at 63x on a Zeiss Microscope oil objective with Zen software (Zeiss Microscopy).

2.9. Statistical analyses

A one-way Analysis of Variance (ANOVA) with a Tukey-Kramer post-hoc test was performed accordingly for experiments. All statistical tests were performed with JMP® Pro software version 13.1.0 (Cary, NC). Statistical significance was considered using a 95% confidence interval ($\alpha=0.05$). For qRT-PCR experiments, gene transcription fold-changes were calculated using the $\Delta\Delta C_T$ method (Livak and Schmittgen, 2001).

3. Results

3.1. PCB-11 exposure concentrations and embryo and larvae body burdens

Zebrafish embryos exposed to either DMSO or 20 μM PCB-11 and their associated aqueous media were analyzed for PCB-11 concentrations at both 28 hpf (4 h after dosing) and at 96 hpf (end of their exposure period). Average PCB-11 concentrations detected in zebrafish media were 61.60 ng/mL at 28 hpf and 37.85 ng/mL at 96 hpf. Average PCB-11 concentrations detected in fish tissue exposed to this media were 400 ng/mg wet weight (ww) at 28 hpf and 1365.4 ng/mg ww at 96 hpf (Table 1). For fish exposed to DMSO, concentrations of PCB-11 remained relatively stable at 0.38 ng/mg ww at 28 hpf and 1.19 ng/mg ww at 96 hpf; media concentrations for these exposures remained stable at 0.19 ng/mL at 28 hpf and 0.20 ng/mL at 96 hpf (Table 1). In comparing the amount of PCB-11 used in the initial dosing concentration (20 μM is 22.5 μg or 22,500 ng per 5 mL in each exposure vial), at 28 hpf 0.89% of this amount was detected in the fish (0.18% per fish), and 1.36% of the initial amount was measured in their associated media. At 96 hpf, of the initial amount of PCB-11 used in the dosing concentration, the percentage of PCB-11 detected in the fish increased to 3.03% (0.61% per fish), and decreased in their associated media to 0.84%.

3.2. PCB-11 alone is a weak agonist of the Ahr

Zebrafish embryos exposed to 0.2 μM , 2 μM , or 20 μM PCB-11 were compared to embryos exposed to a DMSO control for morphology assessments. A small but significant increase from 0.019 mm^2 to 0.029 mm^2 in pericardial area was observed for fish exposed to 20 μM PCB-11, but no other deformities were observed, and no differences in gross morphological development were observed for zebrafish exposed to 0.2 μM or 2 μM PCB-11 (Fig. 1A–B). EROD activity was quantified for each exposure group, and fish exposed to the lowest PCB-11 concentration of 0.2 μM exhibited a significant 45% increase in EROD activity as compared to the DMSO control, whereas 2 μM and 20 μM PCB-11 exhibited no change and a statistically significant decrease of 25%

as compared to the DMSO control, respectively (Fig. 1C). EROD is reflective of Ahr activation and Cyp1a enzyme activity; we compared this EROD data to *ahr2* gene transcription and no differences were observed in any of the exposure groups as compared to the DMSO control (Fig. 1D). For *cyp1a* gene transcription, 0.2 μM and 2 μM PCB-11 did not alter *cyp1a* transcription, however, 20 μM PCB-11 significantly increased *cyp1a* transcription by 2.6-fold (Fig. 1E).

3.3. PCB-11 is an antagonist of the Ahr

A wide variety of chemical structures can interact with the Ahr, and in different contexts act as partial antagonists and/or agonists. To determine whether PCB-11 could function as an antagonist, we designed a co-exposure experiment with a well-studied and potent Ahr agonist, PCB-126. Exposure of zebrafish embryos to 5 nM PCB-126 produces severe cranio-facial, heart, and cardiovascular deformities, which are dependent on *ahr2* (Billiard et al., 2006; Jonsson et al., 2012) and correlate with gene transcription and enzyme activity of Cyp1a. We co-exposed embryos to 5 nM PCB-126 and either 0.2 μM , 2 μM , or 20 μM PCB-11 beginning at 24 hpf and compared these groups to single exposures of DMSO and PCB-126. At 96 hpf, gross morphological deformities and EROD activity for zebrafish co-exposed to PCB-126 and PCB-11 at the 0.2 μM and 2 μM concentrations did not differ from zebrafish exposed to PCB-126 alone; the EROD activity for these exposure groups significantly exceeded the DMSO control group by 470–678% (Fig. 2A). However, 20 μM PCB-11 prevented EROD activity and gross morphological deformities normally induced by PCB-126 so that the EROD activity and morphology for this co-exposed group resembled the DMSO control group (Fig. 2A–C).

We examined *ahr2* and *cyp1a* gene transcription levels for the 20 μM PCB-11 co-exposure group, and compared these results to single exposures of DMSO, 20 μM PCB-11, and 5 nM PCB-126. PCB-126 significantly increased *ahr2* 1.7-fold, the PCB-11 + PCB-126 co-exposure significantly increased *ahr2* 1.6-fold, and PCB-11 alone upregulated *ahr2* a non-statistically significant 1.3-fold (Fig. 2D). For *cyp1a*, gene transcription for fish exposed to 20 μM PCB-11 alone was upregulated 2.4-fold, though this was not statistically significant (Fig. 2E). PCB-126 significantly upregulated *cyp1a* 138-fold, and was reduced to 69-fold in fish co-exposed to 20 μM PCB-11 and PCB-126 (Fig. 2E).

3.4. PCB-11 inhibits Cyp1a activity

In previous co-exposure studies with Ahr agonists that are substrates for Cyp1a metabolism, inhibition of Cyp1a activity has been shown to potentiate activation of the Ahr and enhance embryo deformities (Billiard et al., 2006; Timme-Laragy et al., 2007). To determine whether reduced EROD activity observed in the PCB-

Table 1
PCB-11 fish and media concentrations.

	Unit	Replicate 1	Replicate 2	Replicate 3	Mean	sd	CV
Fish DMSO: 28 hpf	ng/mg	0.39	0.37	0.39	0.38	0.01	3.31%
Fish DMSO: 96 hpf	ng/mg	1.07	1.44	1.04	1.19	0.22	18.4%
Fish PCB11:28 hpf	ng/mg	675	254	271	400	238	59.6%
Fish PCB11:96 hpf	ng/mg	579	1,620	1,900	1,370	695	50.9%
Water DMSO:28 hpf	ng/mL	0.16	0.19	0.20	0.19	0.02	10.0%
Water DMSO:96 hpf	ng/mL	0.24	0.17	0.19	0.20	0.04	18.3%
Water PCB11: 28 hpf	ng/mL	86.1	53.3	45.4	61.6	21.6	35.0%
Water PCB11: 96 hpf	ng/mL	35.3	32.0	46.3	37.9	7.46	19.7%

Note: Fish exposed to either DMSO or 20 μM PCB-11 and their associated media were analyzed for PCB-11 concentrations at both 28 hpf (several hours after dosing) and at 96 hpf (end of their exposure period); fish concentration units are per wet weight. Each replicate and the mean concentration is listed, with sd = standard deviation and CV = coefficient of variation.

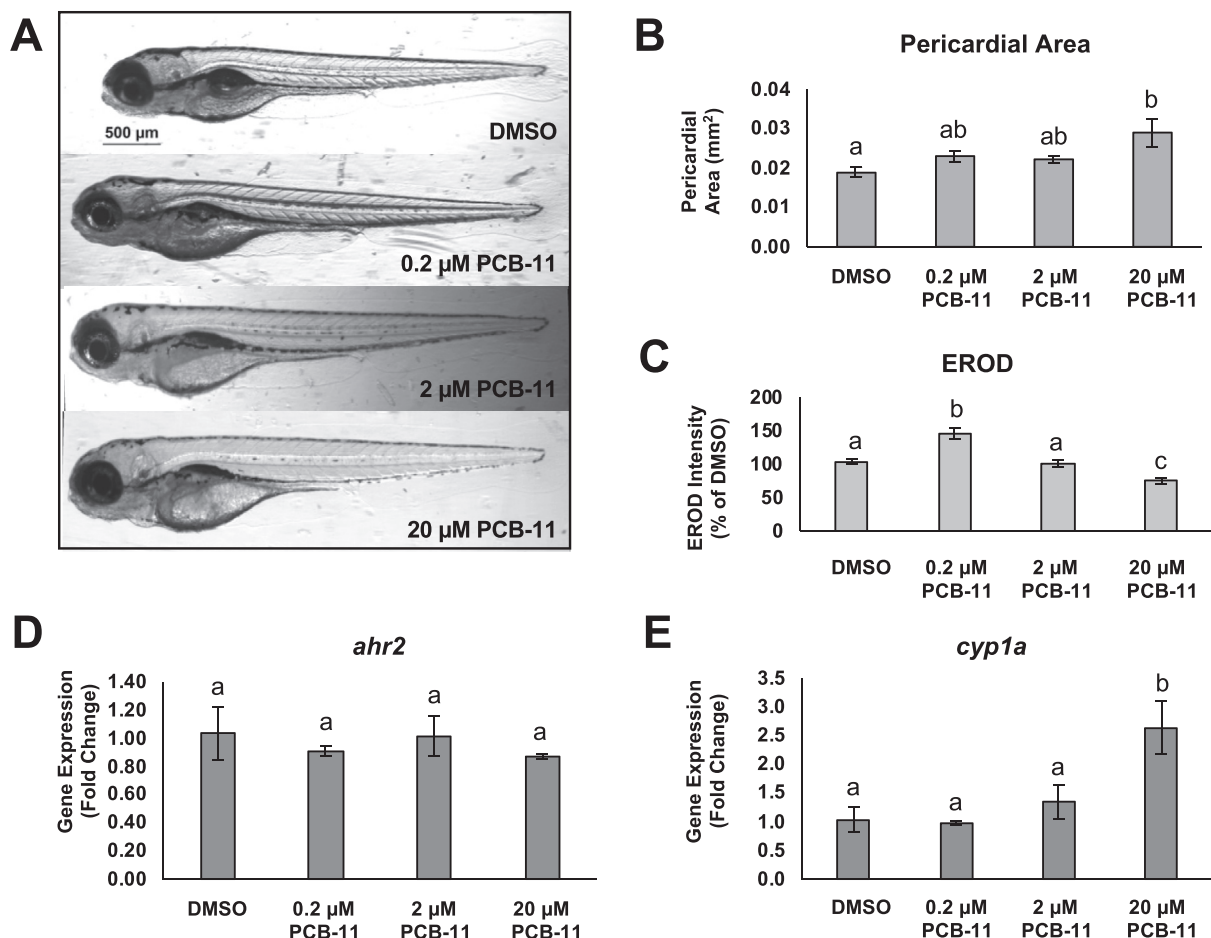


Fig. 1. Single exposures to PCB-11 at 96 hpf. (A) Representative images of zebrafish larvae exposed to DMSO or single concentrations of PCB-11, (B) pericardial area, and (C) EROD activity for each exposure group (mean \pm SEM, $n = 42$ – 43 fish per exposure group across 3 experiments, ANOVA with a Tukey post-hoc test, $p < 0.05$). (D) Gene transcription for DMSO or single exposures of PCB-11 for *ahr2* and (E) *cyp1a* (mean \pm SEM, $n = 3$ – 4 pooled samples of 15 fish per pool per group, ANOVA with Tukey's post-hoc test, $p < 0.05$).

126 experiment was due solely to changes in gene transcription or whether the enzyme action was being impaired, we used a model PAH, BNF, that has previously been shown to exhibit synergistic embryotoxicity upon Cyp1a enzyme inhibition via potentiated activation of the Ahr (Billiard et al., 2006; Timme-Laragy et al., 2007). We originally used a BNF concentration of 367 nM, but this concentration in co-exposures with 20 μ M PCB-11 resulted in 80% mortality (Supplemental Fig. 1). Therefore, we lowered the BNF concentration to 184 nM and repeated this experiment, with all subsequent BNF co-exposures with 20 μ M PCB-11 yielding full survival.

Zebrafish were exposed to 0.2 μ M, 2 μ M, or 20 μ M PCB-11 in combination with 184 nM BNF between 24 and 96 hpf and compared to zebrafish exposed to DMSO or 184 nM BNF alone. At 96 hpf, EROD activity for larvae co-exposed to BNF and either 0.2 μ M or 2 μ M PCB-11 resembled the EROD activity of larvae exposed only to BNF, with all groups having significantly elevated EROD activity of more than 200% greater than DMSO EROD activity but with normal morphological development (Fig. 3A–C). In contrast, 20 μ M PCB-11 reduced the EROD activity of fish in co-exposures with BNF to resemble the EROD activity of the DMSO group, but this co-exposure group experienced significant gross morphological deformities (Fig. 3A–C). To validate these observations, we examined *ahr2* and *cyp1a* gene transcription at 96 hpf for this co-exposure group and compared it to DMSO, 20 μ M PCB-11,

and BNF single exposure groups. BNF significantly upregulated *ahr2* transcription 1.2-fold; this transcription in co-exposures with PCB-11 was reduced to 0.91-fold and was not statistically different than the DMSO exposure group (Fig. 3D). For *cyp1a*, gene transcription for fish exposed to 20 μ M PCB-11 alone was upregulated 3.3-fold in fish, but this was not significant (Fig. 3E). BNF significantly upregulated *cyp1a* 19-fold, and this transcription was reduced to 13-fold in fish co-exposed to 20 μ M PCB-11 and 184 nM BNF (Fig. 3E).

3.5. PCB-11 alters the transcription of genes involved in xenobiotic metabolism, liver development, and endocrine hormone signaling activity

To assess whether PCB-11 affects the transcription of genes outside of the Ahr pathway, we performed RNAseq on the 20 μ M PCB-11 exposure group. After alignment and transcript assembly with the Illumina Tuxedo suite on the Illumina BaseSpace platform, 372 genes were found to be differentially expressed, and of these differentially expressed genes (DEGs), 19 were up-regulated and 18 were down-regulated by more than 2-fold (Table 2). Of these genes, *cyp1a* was upregulated 2.35-fold (data not shown), consistent with *cyp1a* upregulation we observed in our qRT-PCR data of between 2.64 and 3.25-fold, and *jund*, involved in drug response, was downregulated more than 2-fold. In addition to xenobiotic

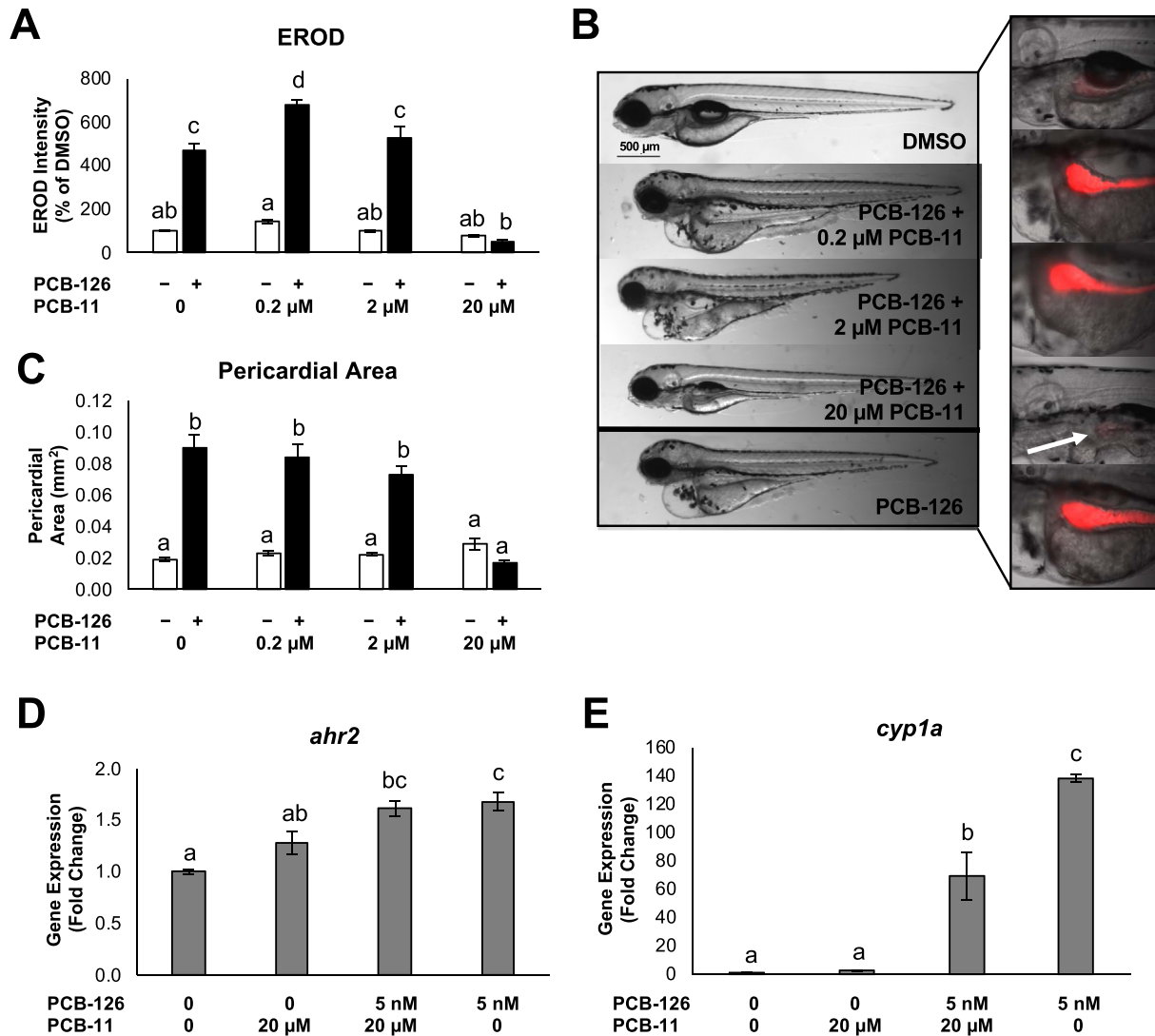


Fig. 2. PCB-11 and PCB-126 co-exposures at 96 hpf. (A) EROD activity for single exposures of PCB-11 (white bars) and co-exposures with PCB-126 (black bars), (B) representative images of EROD activity (red), and (C) pericardial area for single exposures of PCB-11 (white bars) and co-exposures with PCB-126 (black bars). For (A) and (C), single and co-exposure experiments were performed separately, standardized to their respective DMSO groups, and analyzed together (mean \pm SEM, $n = 42$ – 43 fish per group) for single exposure experiments across 3 experiments, $n = 24$ – 28 fish per group for co-exposure experiments across 3 experiments, ANOVA with Tukey's post-hoc test, $p < 0.05$). (D) Gene transcription for DMSO, 20 μ M PCB-11, a 20 μ M PCB-11 + 5 nM PCB-126 co-exposure, and 5 nM PCB-126 quantified for *ahr2* and (E) *cyp1a* (mean \pm SEM, $n = 3$ – 4 pooled samples of 10 fish per pool per group, ANOVA with Tukey's post-hoc test, $p < 0.05$). (For interpretation of the references to colour in this figure legend, the reader is referred to the Web version of this article.)

metabolism DEGs, the genes *lrp5* and *lipca*, involved in liver development and lipid metabolism, were significantly down- and up-regulated, respectively, more than 2-fold. The parathyroid hormone 1a gene, *pth1a*, was upregulated 6.19-fold (data not shown), and the related genes involved in calcium ion binding *oc90* and *s100b* were upregulated and *celsr2* downregulated, all more than 2-fold. Additional information on unannotated DEGs can be found in Supplemental Table 3.

The GSEA platform was used for pathway analysis, using the Kyoto Encyclopedia of Genes and Genomes (KEGG) database. Upon initial analysis, 22 of 135 gene sets were upregulated and 113 of 135 gene sets were downregulated. Under conditions of a nominal p -value of 0.05 and an FDR q -value of 0.20, no gene sets were significantly upregulated, but 14 gene sets were significantly downregulated (Table 2). While some of these gene sets are involved in xenobiotic metabolism and hormone signaling, several of these gene sets such as Sphingolipid Metabolism,

Phosphatidylinositol Signaling System, Fatty Acid Metabolism, and the Adipocytokine Signaling Pathway, are related to lipid signaling and lipid metabolism (Table 2). Gene ontology and pathway analysis was run in parallel on the LRpath platform for comparison, and 35 pathways were significantly up and down-regulated under the same p -value and FDR q -value conditions (Supplemental Table 4). Several of the down-regulated pathways overlap between the two analyses, specifically pathways involved in lipid metabolism. It is known that higher-chlorinated PCBs can disrupt lipid homeostasis (Crawford et al., 2019) but little research has investigated the role of lower-chlorinated PCBs on hepatic function (Umannova et al., 2008).

3.6. PCB-11 impedes liver development and increases vacuole formation in hepatocytes

Based on our previous findings that 20 μ M PCB-11 affects the

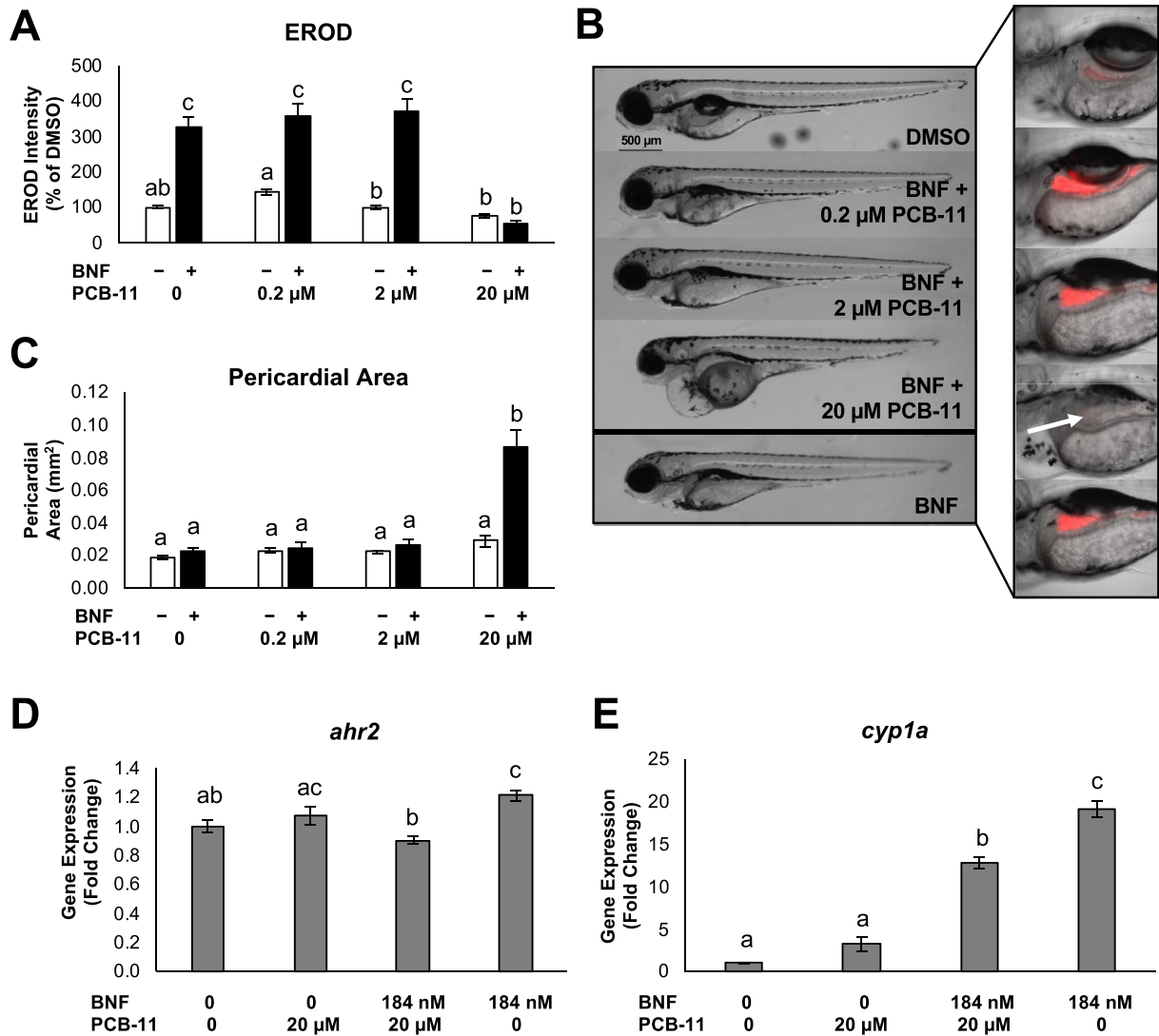


Fig. 3. PCB-11 and BNF co-exposures at 96 hpf. (A) EROD activity for single exposures of PCB-11 (white bars) and co-exposures with BNF (black bars), (B) representative images of EROD activity (red) in gut regions, and (C) pericardial area for single exposures of PCB-11 (white bars) and co-exposures with BNF (black bars). For (A) and (C), single and co-exposure experiments were performed separately, standardized to their respective DMSO groups, and analyzed together (mean \pm SEM, $n = 42\text{--}48$ fish per group for single exposure experiments across 3 experiments, $n = 12\text{--}16$ fish per group for co-exposure experiments across 3 experiments, ANOVA with Tukey's post-hoc test, $p < 0.05$). (D) Gene transcription for DMSO, 20 μM PCB-11, a 20 μM PCB-11 + 50 $\mu\text{g/L}$ BNF co-exposure, and 184 nM BNF quantified for *ahr2* and (E) *cyp1a* (mean \pm SEM, $n = 4\text{--}7$ pooled samples of 10 fish per pool per group, ANOVA with Tukey's post-hoc test, $p < 0.05$). (For interpretation of the references to colour in this figure legend, the reader is referred to the Web version of this article.)

Ahr pathway and in the RNAseq results also affects several pathways related to hepatic functioning, we used the transgenic *Tg(gut:GFP)* zebrafish to examine how PCB-11 affects liver development at 96 hpf. This is a time point consistent with our previous experiments, and a stage during which zebrafish livers are elongating ventrally during development into a functioning hepatic system. At 96 hpf, zebrafish livers in the DMSO, 0.2 μM , and 2 μM PCB-11 exposure groups reached full extension ventrally, but zebrafish livers in the 20 μM PCB-11 exposure group were impeded in their growth and significantly smaller at an average of 0.027 mm^2 compared to an average of 0.033 mm^2 for zebrafish livers in the DMSO exposure group (Fig. 4A–B). No differences in overall growth were observed between exposure groups (data not shown). The livers of fish exposed to either DMSO or 20 μM PCB-11 dose were also examined using histology. Sagittal sections from the midlines of each fish were compared, and sections from the 20 μM PCB-11 exposure group were observed to have greater

vacuolization and fewer numbers of hepatocytes per area of liver tissue as compared to sections from the DMSO exposure group (Fig. 4C).

4. Discussion

This study is, to our knowledge, the first assessment of embryotoxicity of PCB-11 in the zebrafish model. We show here that exposure to PCB-11 can affect liver development, act as a partial agonist/antagonist of the Ahr pathway, and act as an antagonist of Cyp1a activity to modify the toxicity of compounds that interact with the Ahr pathway. Overall, these data provide insight into predicting embryotoxicity of acute exposures to PCB-11.

The concentrations used in the present study ranged from those that were similar to rodent toxicity studies (high concentration, 20 μM , or 4,500 $\mu\text{g/L}$) (Grimm et al., 2015; Sethi et al., 2017) and an environmentally relevant concentration (low concentration,

Table 2
RNAseq Data. 372 differentially expressed genes were identified, with nineteen upregulated and eighteen downregulated more than 2-fold. Genes with an * are annotated with the ENSEMBL gene name from the most recent zebrafish genome build. All 12,935 genes and their log₂ FPKM values were submitted for evaluation using GSEA software programmed for the KEGG Pathway gene set, and the pathways downregulated with a nominal p-value <0.05 and an FDR q-value <0.20 are listed.

Genes upregulated >2-fold		Genes downregulated >2-fold	
<i>zp3a.2</i>	<i>paplnb</i>	<i>zgc:92590</i>	<i>jund</i>
<i>pth1a</i>	<i>npc</i>	<i>baz2a</i>	<i>klf4</i>
* <i>arf4</i>	<i>oc90</i>	<i>celsr2</i>	<i>lama2</i>
<i>he1b</i>	<i>cyp1a</i>	<i>fosab</i>	<i>nrp</i>
<i>m7sk</i>	<i>ndrg1b</i>	<i>acs2l</i>	<i>lrp5</i>
<i>pimr110</i>	<i>tfc2l1</i>	<i>npas4a</i>	<i>opn1lw1</i>
<i>g0s2</i>	<i>npvf</i>	<i>jph1a</i>	<i>fscn2a</i>
<i>urp2</i>	<i>s100b</i>	<i>csf1ra</i>	<i>wwtr1</i>
* <i>crygm1b</i>	<i>lipca</i>	<i>zgc:109982</i>	<i>plac8.1</i>
* <i>rbp1</i>			

GSEA Downregulated KEGG Pathway	Nominal p-value	FDR q-value
Sphingolipid Metabolism	0.042	0.172
Calcium Signaling Pathway	0.034	0.172
Phosphatidylinositol Signaling System	0.029	0.176
Acute Myeloid Leukemia	0.043	0.177
Tight Junction	0.044	0.180
Basal Cell Carcinoma	0.028	0.181
Alanine Aspartate and Glutamate Metabolism	0.043	0.182
Fatty Acid Metabolism	0.038	0.182
Melanogenesis	0.035	0.186
Vascular Smooth Muscle Contraction	0.033	0.186
ERBB Signaling Pathway	0.025	0.188
Adipocytokine Signaling Pathway	0.031	0.192
Adherens Junction	0.046	0.193
Inositol Phosphate Metabolism	0.037	0.194

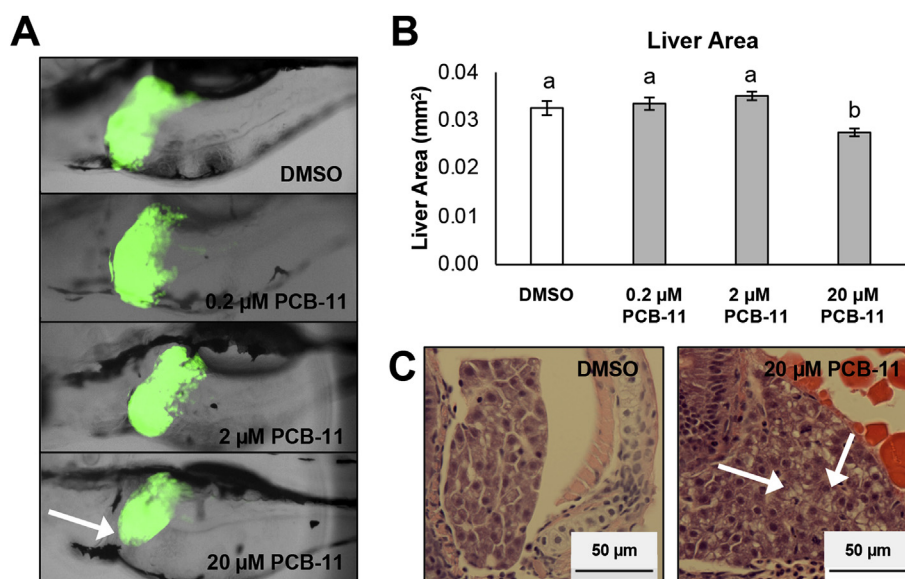


Fig. 4. Liver Development at 96 hpf. (A) Representative images of liver area fluorescing GFP, and (B) quantified for each exposure group (mean \pm SEM, n = 32–43 fish per exposure group across 4 experiments, ANOVA with Tukey's post-hoc test, p < 0.05). (C) Representative images of liver histology sections for zebrafish exposed to DMSO or 20 μ M PCB-11 show more vacuoles in livers of PCB-11 exposed fish (H&E stained, n = 4 fish per exposure group).

0.2 μ M, or 45 μ g/L). This low concentration is still several orders of magnitude higher than environmental concentrations we have observed in water downstream of a paper recycling facility (Supplemental Method 3, Supplemental Fig. 2, and Supplemental Table 5), though it is closer to concentrations that other studies have recorded (Supplemental Table 6). Although our high exposure concentration of 20 μ M (and 61.60 ng/mL detected in the media at 28 hpf) is greater than aquatic concentrations reported to date, it is important to note that much of the compound was not retained in the water or absorbed by the embryo. Four hours after the start of

the exposure, only 0.89% of the initial PCB-11 administered to zebrafish water was detected in the embryos (0.18% per embryo and 1.36% in the associated media at 28 hpf); 72 h after the exposure began these percentages increased to 3.03% in developing larvae (0.61% per larvae) and decreased to 0.84% in the associated media at 96 hpf. Thus, most of the compound likely sorbed to the glass vessel or volatilized before our first sample collection time point at 4 h after exposure. At the stages examined in this study, zebrafish do not yet have a functioning open gut excretion mechanism (Strahle et al., 2012), so while developing larvae may partially metabolize

PCB-11 they absorb, those metabolites would accumulate in their body. Additional research is needed to examine the toxicokinetics of PCB-11. Despite the large reduction from the initial 20 μM PCB-11 dosing concentration, these data indicate both the volatile nature of lower chlorinated PCBs as well as their ability to accumulate in tissue.

The small PCB-11 percentage that entered zebrafish tissue impacted developing zebrafish in exposures to PCB-11 alone (Fig. 1) and in co-exposures with other Ahr agonists. Our results showing 20 μM PCB-11 inhibits Ahr pathway activation in co-exposures with PCB-126 (Fig. 2) is consistent with findings reported for lower-chlorinated PCB co-exposure studies in cell culture (Brennerova et al., 2016; Suh et al., 2003; Takeuchi et al., 2017). Interestingly, we also observed that 20 μM PCB-11 significantly reduces Cyp1a metabolizing activity in co-exposures with BNF and results in severe toxicological outcomes (Fig. 3). We would expect that any substrate not metabolized would continue to activate the Ahr synergistically, consistent with previous studies testing Ahr pathway induction in combination with Cyp1a enzyme inhibition (Billiard et al., 2006; Timme-Laragy et al., 2007); however, we did not observe a synergistic *cyp1a* response. If the morphological deformities observed are indeed mediated through *ahr2*, we would expect that *ahr2* knock-down would rescue these deformities (Jonsson et al., 2007a). Another research group tested this hypothesis with weak Ahr agonists in combination with the PAH fluoranthene, however, knocking down *ahr2* failed to rescue toxicity (Brown et al., 2016). If this is the case for PCB-11, then it is possible that the observed toxicity from PCB-11's antagonistic activity on Cyp1a is mediated through another mechanism. For example, *ahr1a* has been implicated in toxicity response (Garner et al., 2013), though its complete function requires further characterization.

In addition to PCB-11's effects on the Ahr pathway, the RNAseq data for this study highlights its effects on genes and pathways involved in hormone signaling, xenobiotic metabolism, and lipid metabolism. Similar to the PCB-11 single exposure experiments we conducted to observe gross morphology and EROD activity, the effects observed from the RNAseq experiment were modest. Additionally, while 19 genes were significantly up-regulated more than 2-fold, none of these genes besides *cyp1a* have been identified as downstream targets of *ahr2* transcriptional activity, supporting the idea that PCB-11 is only a partial Ahr agonist/antagonist, and influences other gene targets and outcomes. Of these 19 up-regulated genes and the 18 significantly down-regulated genes, pathway analysis using GSEA with an FDR q-value cut-off of 0.20 resulted in no pathways being significantly up-regulated and only 14 KEGG pathways as significantly down-regulated (Table 2). Despite these results, down-regulation of Tight Junction-related genes could result in a degradation of protective barriers in the presence of xenobiotics (Basler et al., 2016), and down-regulation of the ERBB Signaling Pathway, which regulates a family of receptor tyrosine kinases governing diverse biological functions, has been implicated in adverse cardiac development (Chan et al., 2002); we observed in our single exposure experiment mild pericardial edema in response to 20 μM PCB-11. Additionally, the Calcium Signaling Pathway was significantly down-regulated and is important in hormone regulation, cell fate decisions, and more recently has been implicated in liver injury and regeneration (Oliva-Vilarnau et al., 2018). Pathway analysis using LPath was performed for comparative purposes (Supplemental Table 4). This analysis yielded many more significant results using the same parameters as the GSEA analysis, with several overlapping down-regulated pathways related to lipid metabolism. Overall, given that the parameters used for the pathway analyses were not conservative, the results provide modest evidence as to how single

exposures of PCB-11 can affect the pathways discussed previously. Since both of these analyses yielded overlapping pathway results related to lipid metabolism, and since our EROD experiments largely reflect activity in the liver, our subsequent experiments explored PCB-11's effects on liver development.

Using the transgenic *Tg(gut:GFP)* zebrafish line, we observed that 20 μM PCB-11 significantly impedes liver development (Fig. 4). In our histology experiment; H&E staining of liver tissue also suggests differences in hepatocyte density and vacuolization between DMSO and 20 μM PCB-11 exposure groups, however, due to a lack of histological samples, we were unable to quantify these results. Zebrafish are increasingly useful for studying liver pathogenesis (Goessling and Stainier, 2016), including the effects of non-dioxin-like PCBs and their metabolites, which we did not measure in this study. For instance, the half-life of PCB-11 is as little as a few minutes compared to up to 9.5 h for its metabolites in the rodent model (Hu et al., 2014); half-lives for PCB-11 and its metabolites in humans is unknown, but both hydroxylated and sulfated metabolites have been detected in human samples (Flor et al., 2016; Grimm et al., 2015; Grimm et al., 2017). It has been shown that lower-chlorinated PCBs can be hydroxylated *in vivo* by Cyp enzymes to initiate hepatocarcinogenesis through direct DNA adduction (Ludewig et al., 2008; Roos et al., 2011; Umannova et al., 2008), but further histological investigation might help elucidate PCB-11's potential role in xenobiotic metabolism disruption and liver pathology.

In our present study of the Ahr in response to PCB-11, we probed Cyp1a enzyme activity, which is classically involved with Phase I xenobiotic metabolism of both endogenous and exogenous substrates such as certain pharmaceutical drugs and aromatic hydrocarbon compounds. However, our investigation does not identify other potentially important Cyp enzymes in xenobiotic metabolism that could be inhibited by PCB-11. Furthermore, our investigation does not include how PCB-11 might affect crosstalk between the Ahr pathway and other mechanisms; for instance, we have previously shown a relationship between the Ahr and the Nrf2 antioxidant signaling pathway (Rousseau et al., 2015), and other studies have identified PCB-11's agonist/antagonist effects on the Ahr as well as on other hormone receptors in rodent cell culture models (Sethi et al., 2018; Takeuchi et al., 2017). The Ahr pathway also has other diverse functions throughout the human body, including roles in immune response and embryogenesis, where antagonism of Ahr function has been demonstrated to enhance maintenance of hematopoietic stem cell populations (Boitano et al., 2010). This suggests that PCB-11's antagonism of Ahr may potentially impact cell fate decisions in diverse target organs. The antagonistic effect of PCB-11 on the Ahr observed in this study therefore emphasizes an important gap in our understanding of the systemic impacts of toxicological and pharmacological mixtures, and highlights important areas of investigation for future studies.

In summary, while higher concentrations of single exposures of PCB-11 has mild effects on development and Ahr function, this work introduces other mechanisms by which PCB-11 may have adverse health consequences. The antagonistic or competitive effect of PCB-11 on Ahr and Cyp1a in the presence of classical agonists suggests that ubiquitous PCB-11 exposures may interact with other toxicants and pharmacological agents acting through these pathways. While this study focused on the effects of acute exposures at higher concentrations, further studies could examine the effects of more environmentally-relevant concentrations under a chronic exposure paradigm. This work also underscores the importance of characterizing the species composition of mixtures in environmental risk assessments, as no organism would be exposed to PCB-11 in the absence of other chemicals, including other PCBs.

5. Conclusions

The environmentally relevant concentration of PCB-11 used for laboratory experiments in this study (0.2 μM) does not appear to cause deviations in embryonic development in the zebrafish model in either single or co-exposures with other Ahr agonists. Of the higher 20 μM PCB-11 concentration tested, 0.61% was absorbed per fish by 96 hpf. In single exposures, this concentration mildly activates the Ahr and results in subtle changes in liver histology and significant decreases in liver size. In addition, this PCB-11 concentration in co-exposures with other Ahr agonists both exacerbates and inhibits embryonic deformities in zebrafish, depending on the agonist, and inhibits Cyp1a activity. As many pharmaceuticals and xenobiotic compounds are metabolized via the Ahr pathway and Cyp family of enzymes, these results suggest that if exposures at this concentration occur, PCB-11 may potentially cause drug interactions or other interferences with xenobiotic metabolism for both aquatic life and humans. Additional studies would help evaluate the effects of co-exposures, outcomes at other life stages, and verify the molecular actions of this emerging contaminant.

Funding

Funding for this work was provided in part by the National Institutes of Health (grant numbers R01ES025748 to ART-L and F32ES028085 to KES), the Iowa Superfund Research Program (ISRP) and the Superfund Research Program of the National Institute of Environmental Health Sciences (grant number P42ES013661 to KCH), and through the UMass Public Service Endowment Grant program (to ART-L). Funding was also provided to MAR through a predoctoral fellowship from the University of Massachusetts Amherst as part of the Biotechnology Training Program (National Research Service Award T32 GM108556).

Declaration of interests

The authors declare that they have no known competing financial interests or personal relationships that could have appeared to influence the work reported in this paper.

Acknowledgements

We would like to acknowledge members of the Timme-Laragy laboratory for providing excellent zebrafish care at UMass Amherst. We thank the Barresi lab at Smith College for assistance with AB embryos, and the UMass Worcester Microscopy Core and Vandenberg lab at UMass Amherst for histology support. We also thank the UMass Amherst Genomics Resource Laboratory, which acknowledges funding support from The Massachusetts Life Sciences Center (MLSC), for their RNA isolation, RNAseq library preparation, and sequencing services. Any use of trade, product, or firm names is for descriptive purposes only and does not imply endorsement by the U.S. Government.

Appendix A. Supplementary data

Supplementary data to this article can be found online at <https://doi.org/10.1016/j.envpol.2019.113027>.

References

Addison, R.F., Ikononou, M.G., Stobo, W.T., 1999. Polychlorinated dibenzo-p-dioxins and furans and non-ortho- and mono-ortho-chlorine substituted polychlorinated biphenyls in grey seals (*Halichoerus grypus*) from Sable Island, Nova Scotia, in 1995. *Mar. Environ. Res.* 47, 225–240.

Agency for Toxic Substances and Disease Registry, 2000. *Toxicological Profile for*

Polychlorinated Biphenyls (PCBs). Agency for Toxic Substances and Disease Registry, Atlanta, Georgia.

Andreasen, E.A., Spitsbergen, J.M., Tanguay, R.L., Stegeman, J.J., Heideman, W., Peterson, R.E., 2002. Tissue-specific expression of AHR2, ARNT2, and CYP1A in zebrafish embryos and larvae: effects of developmental stage and 2,3,7,8-tetrachlorodibenzo-p-dioxin exposure. *Toxicol. Sci.* 68, 403–419.

Basler, K., Bergmann, S., Heisig, M., Naegel, A., Zorn-Kruppa, M., Brandner, J.M., 2016. The role of tight junctions in skin barrier function and dermal absorption. *J. Control. Release* 242, 105–118.

Billiard, S.M., Timme-Laragy, A.R., Wassenberg, D.M., Cockman, C., Di Giulio, R.T., 2006. The role of the aryl hydrocarbon receptor pathway in mediating synergistic developmental toxicity of polycyclic aromatic hydrocarbons to zebrafish. *Toxicol. Sci.* 92, 526–536.

Boehler, S., Lorracher, A.K., Schubert, J., Braunbeck, T., 2018. Comparative live-imaging of in vivo EROD (ethoxyresorufin-O-deethylase) induction in zebrafish (*Danio rerio*) and fathead minnow (*Pimephales promelas*) embryos after exposure to PAHs and river sediment extracts. *Sci. Total Environ.* 621, 827–838.

Boitano, A.E., Wang, J., Romeo, R., Bouchez, L.C., Parker, A.E., Sutton, S.E., Walker, J.R., Flaveny, C.A., Perdev, G.H., Denison, M.S., Schultz, P.G., Cooke, M.P., 2010. Aryl hydrocarbon receptor antagonists promote the expansion of human hematopoietic stem cells. *Science* 329, 1345–1348.

Brenerova, P., Hamers, T., Kamstra, J.H., Vondracek, J., Strapacova, S., Andersson, P.L., Machala, M., 2016. Pure non-dioxin-like PCB congeners suppress induction of AhR-dependent endpoints in rat liver cells. *Environ. Sci. Pollut. Res. Int.* 23, 2099–2107.

Brown, D.R., Clark, B.W., Garner, L.V., Di Giulio, R.T., 2016. Embryonic cardiotoxicity of weak aryl hydrocarbon receptor agonists and CYP1A inhibitor fluoranthene in the Atlantic killifish (*Fundulus heteroclitus*). *Comp. Biochem. Physiol. C Toxicol. Pharmacol.* 188, 45–51.

Carney, S.A., Prasch, A.L., Heideman, W., Peterson, R.E., 2006. Understanding dioxin developmental toxicity using the zebrafish model. *Birth Defect. Res. A Clin. Mol. Teratol.* 76, 7–18.

Chan, R., Hardy, W.R., Laing, M.A., Hardy, S.E., Muller, W.J., 2002. The catalytic activity of the ErbB-2 receptor tyrosine kinase is essential for embryonic development. *Mol. Cell. Biol.* 22, 1073–1078.

Chen, X., Lin, Y., Dang, K., Puschner, B., 2017. Quantification of polychlorinated biphenyls and polybrominated diphenyl ethers in commercial cows' milk from California by gas chromatography-triple quadrupole mass spectrometry. *PLoS One* 12, e0170129.

Coumailleau, P., Poellinger, L., Gustafsson, J.A., Whitelaw, M.L., 1995. Definition of a minimal domain of the dioxin receptor that is associated with Hsp90 and maintains wild type ligand binding affinity and specificity. *J. Biol. Chem.* 270, 25291–25300.

Crawford, K.A., Clark, B.W., Heiger-Bernays, W.J., Karchner, S.I., Claus Henn, B.G., Griffith, K.N., Howes, B.L., Schlezinger, D.R., Hahn, M.E., Nacci, D.E., Schlezinger, J.J., 2019. Altered lipid homeostasis in a PCB-resistant Atlantic killifish (*Fundulus heteroclitus*) population from new Bedford Harbor, MA, U.S.A. *Aquat. Toxicol.* 210, 30–43.

Du, S., Belton, T.J., Rodenburg, L.A., 2008. Source apportionment of polychlorinated biphenyls in the tidal Delaware River. *Environ. Sci. Technol.* 42, 4044–4051.

Dunnivant, F.M., O'pax, p.p.m.p.p.p., Helvetica, f.p., Elzerman, A.W., 1988. Aqueous solubility and Henry's law constant data for PCB congeners for evaluation of quantitative structure-property relationships (QSPRs). *Chemosphere* 17, 16.

Field, H.A., Ober, E.A., Roeser, T., Stainier, D.Y., 2003. Formation of the digestive system in zebrafish. I. Liver morphogenesis. *Dev. Biol.* 253, 279–290.

Flor, S., He, X., Lehmler, H.J., Ludwig, G., 2016. Estrogenicity and androgenicity screening of PCB sulfate monoesters in human breast cancer MCF-7 cells. *Environ. Sci. Pollut. Res. Int.* 23, 2186–2200.

Garner, L.V., Brown, D.R., Di Giulio, R.T., 2013. Knockdown of AHR1A but not AHR1B exacerbates PAH and PCB-126 toxicity in zebrafish (*Danio rerio*) embryos. *Aquat. Toxicol.* 142–143, 336–346.

Goessling, W., Stainier, D.Y., 2016. Endoderm specification and liver development. *Methods Cell Biol.* 134, 463–483.

Goldstone, J.V., Goldstone, H.M., Morrison, A.M., Tarrant, A., Kern, S.E., Woodin, B.R., Stegeman, J.J., 2007. Cytochrome P450 1 genes in early deuterostomes (tunicates and sea urchins) and vertebrates (chicken and frog): origin and diversification of the CYP1 gene family. *Mol. Biol. Evol.* 24, 2619–2631.

Grimm, F.A., He, X., Teesch, L.M., Lehmler, H.J., Robertson, L.W., Duffel, M.W., 2015. Tissue distribution, metabolism, and excretion of 3,3'-Dichloro-4'-sulfoxy-biphenyl in the rat. *Environ. Sci. Technol.* 49, 8087–8095.

Grimm, F.A., Lehmler, H.J., Koh, W.X., DeWall, J., Teesch, L.M., Hornbuckle, K.C., Thorne, P.S., Robertson, L.W., Duffel, M.W., 2017. Identification of a sulfate metabolite of PCB 11 in human serum. *Environ. Int.* 98, 120–128.

Herkert, N.J., Jahnke, J.C., Hornbuckle, K.C., 2018 May 1. Emissions of tetrachlorobiphenyls (PCBs 47, 51, and 68) from polymer resin on kitchen cabinets as a non-aro-clor source to residential air. *Environ. Sci. Technol.* 52 (9), 5154–5160. <https://doi.org/10.1021/acs.est.8b00966>.

Hu, D., Martinez, A., Hornbuckle, K.C., 2008. Discovery of non-aro-clor PCB (3,3'-dichlorobiphenyl) in Chicago air. *Environ. Sci. Technol.* 42, 7873–7877.

Hu, X., Adamcakova-Dodd, A., Thorne, P.S., 2014. The fate of inhaled (14)C-labeled PCB11 and its metabolites in vivo. *Environ. Int.* 63, 92–100.

Huang, Z.J., Edery, I., Rosbash, M., 1993. PAS is a dimerization domain common to *Drosophila* period and several transcription factors. *Nature* 364, 259–262.

International Agency for Research on Cancer, 2016. Polychlorinated Biphenyls and Polybrominated Biphenyls, IARC Monographs on the Evaluation of Carcinogenic

- Risks to Humans. International Agency for Research on Cancer, Lyon, France.
- Jonsson, M.E., Jenny, M.J., Woodin, B.R., Hahn, M.E., Stegeman, J.J., 2007a. Role of AHR2 in the expression of novel cytochrome P450 1 family genes, cell cycle genes, and morphological defects in developing zebra fish exposed to 3,3',4,4',5-pentachlorobiphenyl or 2,3,7,8-tetrachlorodibenzo-p-dioxin. *Toxicol. Sci.* 100, 180–193.
- Jonsson, M.E., Kubota, A., Timme-Laragy, A.R., Woodin, B., Stegeman, J.J., 2012. Ahr2-dependence of PCB126 effects on the swim bladder in relation to expression of CYP1 and cox-2 genes in developing zebrafish. *Toxicol. Appl. Pharmacol.* 265, 166–174.
- Jonsson, M.E., Orrego, R., Woodin, B.R., Goldstone, J.V., Stegeman, J.J., 2007b. Basal and 3,3',4,4',5-pentachlorobiphenyl-induced expression of cytochrome P450 1A, 1B and 1C genes in zebrafish. *Toxicol. Appl. Pharmacol.* 221, 29–41.
- Kais, B., Ottermanns, R., Scheller, F., Braunbeck, T., 2018. Modification and quantification of in vivo EROD live-imaging with zebrafish (*Danio rerio*) embryos to detect both induction and inhibition of CYP1A. *Sci. Total Environ.* 615, 330–347.
- Karchner, S.I., Franks, D.G., Hahn, M.E., 2005. AHR1B, a new functional aryl hydrocarbon receptor in zebrafish: tandem arrangement of ahr1b and ahr2 genes. *Biochem. J.* 392, 153–161.
- Kim, J.H., Karnovsky, A., Mahavisno, V., Weymouth, T., Pande, M., Dolinoy, D.C., Rozek, L.S., Sartor, M.A., 2012. LRpath analysis reveals common pathways dysregulated via DNA methylation across cancer types. *BMC Genomics* 13, 526.
- King-Heiden, T.C., Mehta, V., Xiong, K.M., Lanham, K.A., Antkiewicz, D.S., Ganser, A., Heideman, W., Peterson, R.E., 2012. Reproductive and developmental toxicity of dioxin in fish. *Mol. Cell. Endocrinol.* 354, 121–138.
- Koh, W.X., Hornbuckle, K.C., Thorne, P.S., 2015. Human serum from urban and rural adolescents and their mothers shows exposure to polychlorinated biphenyls not found in commercial mixtures. *Environ. Sci. Technol.* 49, 8105–8112.
- Kuhnert, A., Vogts, C., Seiwert, B., Aulhorn, S., Altenburger, R., Hollert, H., Kuster, E., Busch, W., 2017. Biotransformation in the Zebrafish Embryo -temporal Gene Transcription Changes of Cytochrome P450 Enzymes and Internal Exposure Dynamics of the AhR Binding Xenobiotic Benz[a]anthracene. *Environ Pollut.*, vol. 2017. Elsevier Ltd, England, pp. 1–11.
- Litten, S., Fowler, B., Luszniak, D., 2002. Identification of a novel PCB source through analysis of 209 PCB congeners by US EPA modified method 1668. *Chemosphere* 46, 1457–1459.
- Livak, K.J., Schmittgen, T.D., 2001. Analysis of relative gene expression data using real-time quantitative PCR and the 2^{(-Delta Delta C(T))} Method. *Methods* 25, 402–408.
- Ludewig, G., Lehmann, L., Esch, H., Robertson, L.W., 2008. Metabolic activation of PCBs to carcinogens in vivo - a review. *Environ. Toxicol. Pharmacol.* 25, 241–246.
- Nacci, D., Coiro, L., Wassenberg, D., Di Giulio, R., 2005. A non-destructive technique to measure cytochrome P4501A enzyme activity in living embryos of the estuarine fish *Fundulus heteroclitus*. In: Ostrander, G.K. (Ed.), *Techniques in Aquatic Toxicology*, vol. 2, pp. 209–225.
- Nakayama, A., Riesen, I., Kollner, B., Eppler, E., Segner, H., 2008. Surface marker-defined head kidney granulocytes and B lymphocytes of rainbow trout express benzo[a]pyrene-inducible cytochrome P4501A protein. *Toxicol. Sci.* 103, 86–96.
- Nebert, D.W., Dalton, T.P., Okey, A.B., Gonzalez, F.J., 2004. Role of aryl hydrocarbon receptor-mediated induction of the CYP1 enzymes in environmental toxicity and cancer. *J. Biol. Chem.* 279, 23847–23850.
- Oliva-Vilarnau, N., Hankeova, S., Vorrink, S.U., Mkrtrchian, S., Andersson, E.R., Lauschke, V.M., 2018. Calcium signaling in liver injury and regeneration. *Front. Med.* 5, 192.
- Pizzini, S., Sbicego, C., Corami, F., Grotti, M., Magi, E., Bonato, T., Cozzi, G., Barbante, C., Piazza, R., 2017. 3,3'-dichlorobiphenyl (non-Aroclor PCB-11) as a marker of non-legacy PCB contamination in marine species: comparison between Antarctic and Mediterranean bivalves. *Chemosphere* 175, 28–35.
- Reisz-Porszasz, S., Probst, M.R., Fukunaga, B.N., Hankinson, O., 1994. Identification of functional domains of the aryl hydrocarbon receptor nuclear translocator protein (ARNT). *Mol. Cell. Biol.* 14, 6075–6086.
- Rodenburg, L.A., Du, S., Xiao, B., Fennell, D.E., 2011. Source apportionment of polychlorinated biphenyls in the New York/New Jersey Harbor. *Chemosphere* 83, 792–798.
- Rodenburg, L.A., Guo, J., Du, S., Cavallo, G.J., 2010. Evidence for unique and ubiquitous environmental sources of 3,3'-dichlorobiphenyl (PCB 11). *Environ. Sci. Technol.* 44, 2816–2821.
- Rodenburg, L.A., Krumin, V., Curran, J.C., 2015. Microbial dechlorination of polychlorinated biphenyls, dibenzo-p-dioxins, and -furans at the Portland Harbor Superfund site, Oregon, USA. *Environ. Sci. Technol.* 49, 7227–7235.
- Roos, R., Andersson, P.L., Halldin, K., Hakansson, H., Westerholm, E., Hamers, T., Hamscher, G., Heikkinen, P., Korkalainen, M., Leslie, H.A., Niittynen, M., Sankari, S., Schmitz, H.J., van der Ven, L.T., Viluksela, M., Schrenk, D., 2011. Hepatic effects of a highly purified 2,2',3,4,4',5,5'-heptachlorobiphenyl (PCB 180) in male and female rats. *Toxicology* 284, 42–53.
- Rousseau, M.E., Sant, K.E., Borden, L.R., Franks, D.G., Hahn, M.E., Timme-Laragy, A.R., 2015. Regulation of Ahr signaling by Nrf2 during development: effects of Nrf2a deficiency on PCB126 embryotoxicity in zebrafish (*Danio rerio*). *Aquat. Toxicol.* 167, 157–171.
- Scornaienci, M.L., Thornton, C., Willett, K.L., Wilson, J.Y., 2010. Functional differences in the cytochrome P450 1 family enzymes from zebrafish (*Danio rerio*) using heterologously expressed proteins. *Arch. Biochem. Biophys.* 502, 17–22.
- Sethi, S., Keil, K.P., Chen, H., Hayakawa, K., Li, X., Lin, Y., Lehmler, H.J., Puschner, B., Lein, P.J., 2017 Aug 1. Detection of 3,3'-dichlorobiphenyl in human maternal plasma and its effects on axonal and dendritic growth in primary rat neurons. *Toxicol. Sci.* 158 (2), 401–411. <https://doi.org/10.1093/toxsci/kfx100>.
- Sethi, S., Keil, K.P., Lein, P.J., 2018 Nov. 3,3'-Dichlorobiphenyl (PCB 11) promotes dendritic arborization in primary rat cortical neurons via a CREB-dependent mechanism. *Arch. Toxicol.* 92 (11), 3337–3345. <https://doi.org/10.1007/s00204-018-2307-8>.
- Shanahan, C.E., Spak, S.N., Martinez, A., Hornbuckle, K.C., 2015. Inventory of PCBs in Chicago and opportunities for reduction in airborne emissions and human exposure. *Environ. Sci. Technol.* 49, 13878–13888.
- Shang, H., Li, Y., Wang, T., Wang, P., Zhang, H., Zhang, Q., Jiang, G., 2014. The presence of polychlorinated biphenyls in yellow pigment products in China with emphasis on 3,3'-dichlorobiphenyl (PCB 11). *Chemosphere* 98, 44–50.
- Sojka, K.M., Kern, C.B., Pollenz, R.S., 2000. Expression and subcellular localization of the aryl hydrocarbon receptor nuclear translocator (ARNT) protein in mouse and chicken over developmental time. *Anat. Rec.* 260, 327–334.
- Strahle, U., Scholz, S., Geisler, R., Greiner, P., Hollert, H., Rastegar, S., Schumacher, A., Selderslaghs, I., Weiss, C., Witters, H., Braunbeck, T., 2012. Zebrafish embryos as an alternative to animal experiments—a commentary on the definition of the onset of protected life stages in animal welfare regulations. *Reprod. Toxicol.* 33, 128–132.
- Suh, J., Kang, J.S., Yang, K.H., Kaminski, N.E., 2003. Antagonism of aryl hydrocarbon receptor-dependent induction of CYP1A1 and inhibition of IgM expression by di-ortho-substituted polychlorinated biphenyls. *Toxicol. Appl. Pharmacol.* 187, 11–21.
- Takeuchi, S., Anezaki, K., Kojima, H., 2017. Effects of unintentional PCBs in pigments and chemical products on transcriptional activity via aryl hydrocarbon and nuclear hormone receptors. *Environ. Pollut.* 227, 306–313.
- Timme-Laragy, A.R., Cockman, C.J., Matson, C.W., Di Giulio, R.T., 2007. Synergistic induction of AHR regulated genes in developmental toxicity from co-exposure to two model PAHs in zebrafish. *Aquat. Toxicol.* 85, 241–250.
- Umanova, L., Neca, J., Andrysik, Z., Vondracek, J., Upham, B.L., Trosko, J.E., Hofmanova, J., Kozubik, A., Machala, M., 2008. Non-dioxin-like polychlorinated biphenyls induce a release of arachidonic acid in liver epithelial cells: a partial role of cytosolic phospholipase A(2) and extracellular signal-regulated kinases 1/2 signalling. *Toxicology* 247, 55–60.
- Wincent, E., Kubota, A., Timme-Laragy, A., Jonsson, M.E., Hahn, M.E., Stegeman, J.J., 2016. Biological effects of 6-formylindolo[3,2-b]carbazole (FICZ) in vivo are enhanced by loss of CYP1A function in an Ahr2-dependent manner. *Biochem. Pharmacol.* 110–111, 117–129.
- Zhao, B., Bohonowych, J.E., Timme-Laragy, A., Jung, D., Affatato, A.A., Rice, R.H., Di Giulio, R.T., Denison, M.S., 2013. Common commercial and consumer products contain activators of the aryl hydrocarbon (dioxin) receptor. *PLoS One* 8, e56860.
- Zhu, C., Wang, P., Li, Y., Chen, Z., Li, W., Ssebugere, P., Zhang, Q., Jiang, G., 2015. Bioconcentration and trophic transfer of polychlorinated biphenyls and polychlorinated dibenzo-p-dioxins and dibenzofurans in aquatic animals from an e-waste dismantling area in East China. *Environ. Sci. Process Impacts* 17, 693–699.